Received: 19 December 2017 | Revised: 29 April 2018 | Accepted: 5 May 2018

DOI: 10.1002/dac.3720

RESEARCH ARTICLE

WILEY

Error performance of Uncoded Space Time Labelling Diversity in spatially correlated Nakagami-q channels

Sulaiman Saleem Patel | Tahmid Quazi | Hongjun Xu

School of Engineering, University of Kwa-Zulu Natal, Durban, South Africa

Correspondence
Sulaiman Saleem Patel, School of Engineering, University of Kwa-Zulu Natal, Durban, South Africa.
Email: sulaiman.s.patel@gmail.com

Summary

Greater spectral efficiency has recently been achieved for Uncoded Space Time Labelling Diversity (USTLD) systems by increasing the number of antennas in the transmit antenna array. However, due to constrained physical space in hardware, the use of more antennas can lead to degradation in error performance due to correlation. Thus, this paper studies the effects of spatial correlation on the error performance of USTLD systems. The union bound approach, along with the Kronecker correlation model, is used to derive an analytical expression for the average bit error probability (ABEP) in the presence of Nakagami-*q* fading. This expression is validated by the results of Monte Carlo simulations, which shows a tight fit in the high signal-to-noise ratio (SNR) region. The degradation in error performance due to transmit and receive antenna correlation is investigated independently. Results indicate that transmit antenna correlation in the USTLD systems investigated (3×3 8PSK, 2×4 16PSK, 2×4 16QAM, and 2×4 64QAM) causes a greater degradation in error performance than receive antenna correlation. It is also shown that 2×4 USTLD systems are more susceptible to correlation than comparable space-time block coded systems for 8PSK, 16PSK, 16QAM, and 64QAM.

KEYWORDS

correlated channels, Hoyt, labelling diversity, MIMO, Nakagami-q

1 | INTRODUCTION

The idea of labelling diversity was initially proposed by Huang and Ritcey[1,2] for bit-interleaved coded systems with iterative decoding (BICSs-ID), which was later expanded on by Krasicki.[3,4] The use of convolutional coding in BICSs-ID incurs high detection complexity, resulting in higher latencies and increased power consumption. This motivated for the subsequent application of labelling diversity to uncoded systems, such as decode-and-forward relay systems,[5] multi-packet data transmissions with automatic repeat requests,[6,7] space-time block coded (STBC) systems,[8] STBC systems with spatial modulation,[9] and space time channel modulated STBC systems using radio frequency mirrors. [10]

The focus of this paper is on the Uncoded Space Time Labelling Diversity (USTLD) systems proposed by Xu et al.[8] USTLD systems achieve improved error performance compared with conventional multiple-input, multiple-output (MIMO) systems as a result of 2 diversity mechanisms: labelling diversity and antenna diversity. Labelling diversity is achieved by transmitting the same binary data over 2 time slots using symbols from 2 different constellation mappings. The binary mappers are designed such that adjacent symbols in each constellation map are spaced further apart in subsequent maps. This allows detection to be based on symbol pairs instead of individual symbols. In doing so, error

performance is improved in a similar manner to conventional error correction codes,[11] despite USTLD being an uncoded system.

Antenna diversity is achieved by adopting a MIMO structure, which creates more signal paths between transmitter and receiver, each of which experiences independent fading. Ideally, these signal paths are independent and identically distributed (iid). The use of multiple signal paths leads to lower error rates when compared with a single path.[11,12] The original MIMO structure of USTLD[8] describes a system with 2 transmit antennas and any arbitrary N_r receive antennas. This $2 \times N_r$ structure, along with the use of 2 time slots to transmit the same binary information, closely resembles the orthogonal STBC system proposed by Alamouti.[13] Xu et al show that labelling diversity allows USTLD systems to achieve better error performance than Alamouti STBC systems.

The $2 \times N_r$ USTLD model was recently extended to consider any arbitrary N_t transmit antennas by Patel et al.[14] It is noted that $N_t \times N_r$ USTLD systems are comparable to existing quasi-orthogonal STBC (Q-STBC) systems with more than 2 transmit antennas. [15-17] The use of $N_t > 2$ transmit antennas allows Q-STBC systems to achieve more transmit antenna diversity, improving error performance. However, Q-STBC systems use more than 2 time slots to transmit the same binary information. As a result, Q-STBC systems experience higher latencies, decreased spectral efficiency and increased processing overheads. $N_t \times N_r$ USTLD systems are not as affected by these challenges as they use only 2 time slots.

Conventional ideal analysis of MIMO systems, such as USTLD, assumes that signal paths are iid, and hence, the channels are uncorrelated. However, in a real system, channels may experience spatial or temporal correlation. Temporal correlation arises when the system experiences deep fading.[12,18] Spatial correlation results from the physical proximity of antennas and may be expressed as a function of the spacing between antennas and the wavelength of the transmission carrier.[19-21] Due to the inverse proportionality between wavelength and frequency, there is a greater likelihood of antenna correlation occurring at higher frequencies (such as the millimetre wave frequency spectrum that has been studied for next-generation MIMO systems.[22]) To this end, the study of USTLD in spatially correlated channels provides insight into the degradation in error performance that may be expected when USTLD is applied to real systems, such as mobile ad hoc networks or satellite telecommunication. Temporal correlation is not studied in detail, as the error performance of USTLD does not degrade in the presence of quasi-static fading across both transmission time slots. [8]

The simplest case of correlated channel analysis is to consider a system with dual-correlated receive antennas (i.e. 2 correlated receive antennas). In Fang et al,[23] it is shown that identical, dual-correlated channels may be modelled as equivalent nonidentical, uncorrelated channels by applying an orthogonal transform. This technique was adapted in a study of USTLD systems in dual-correlated channels,[24] which presents results for a 2×2 system assuming no transmit antenna correlation. The same work[24] also shows that, for dual-correlated systems, the error performance of USTLD deteriorates more rapidly as channel correlation increases when compared with conventional MIMO systems.

This paper extends the aforementioned study[24] to the more general case of $N_t \times N_r$ USTLD systems in the presence of antenna correlation, at either the transmit or receive sides, or both. To achieve this, the methods of analysis given in Hedayet et al[18] are adopted in this paper. By using the Kronecker model,[25] Hedayet et al shows that the identical correlated channels of space-time coded MIMO systems may be modelled as eigenvalue-weighted, uncorrelated channels for statistical analysis.[18] This technique has previously been employed in the study of various other correlated MIMO systems such as space-time trellis coded systems,[18] super-orthogonal space-time trellis coded systems,[18] generalised STBC systems,[18] STBC spatial modulation systems,[26] decode-and-forward based cooperative STBC spatial modulation system,[27] linear dispersion coded systems, [18] and diagonal-algebraic space-time coded systems.[18] It is noted that other correlation models have been proposed in literature, such as the nonseparable correlation model.[28-31] These studies indicate that the nonseparable model provides a better fit to measured data than the Kronecker model when analysing channel capacity. However, the works of Tulino et al,[29] Lin et al,[32] and Moustakas et al[33] show that the nonseparable model reduces to the Kronecker model for systems that achieve antenna diversity, and hence, they are equivalent for USTLD systems.

Previous studies of USTLD[8,14,24] have all been conducted under the assumption of Rayleigh fading channels. The Rayleigh fading model describes transmission paths where there is no strong line-of-sight path between the transmitter and receiver.[11,12] A more general model that better indicates the worst-case performance of a MIMO system is the Nakagami-q fading model,[34,35] which encompasses Rayleigh fading as a specific case. Literature shows that Nakagami-q provides a good fit for modelling signal propagation in satellite links subjected to strong ionospheric scintillation. [12,36] To this end, a further contribution of this paper is that the error performance of USTLD is derived for Nakagami-q.

In terms of notation, this paper represents vectors and matrices in boldface and scalars in italics. $(\cdot)^{\mathrm{T}}$, $(\cdot)^{\mathrm{H}}$, $\|\cdot\|$ and $\mathcal{E}\{\cdot\}$ represent the transpose, Hermitian operator, vector Frobenius norm, and statistical expectation, respectively. $J_0(z)$ and $I_0(z)$ are the respective unmodified and modified zeroth-order Bessel functions of the first kind, related by $J_0(z) = I_0(-\mathrm{j}z)$, as indicated by Weisstein.[37] $a \sim \mathcal{N}(\bar{x}, \sigma^2)$ means that the random variable a follows a normal distribution with mean $\bar{x}$ and variance σ^2. The superscripts $(\cdot)^{\mathrm{I}}$ and $(\cdot)^{\mathrm{Q}}$ represent the in-phase and quadrature components of complex signals, respectively. The operator $\mathcal{V}\{\mathbf{A}\}$ returns the eigenvalues of matrix $\mathbf{A}$.

2 | SYSTEM MODEL

2.1 | Transmission model

The system considers an $N_t \times N_r$ USTLD system as defined by Patel et al,[14] where $N_t \leq N_r$. For a 2^m-ary constellation, every m bits from the data stream defines a codeword, or "label," L. Thus, a bitstream of mN_t information bits produces a label vector with N_t entries, $\mathbf{L} = [L_1 \ \cdots L_{N_t}]^{\mathrm{T}}$. $\mathbf{L}$ is used to produce symbols that are transmitted across 2 time slots. To achieve labelling diversity, the transmitted symbols in each time slot are selected from different binary mappers Ω_1 and Ω_2. The vector of symbols transmitted in time slot k, where $k \in [1{:}2]$, is thus $[\Omega_k(\mathbf{L})] = [\Omega_k(L_1) \ \cdots \Omega_k(L_{N_t})]^{\mathrm{T}}$. This work focuses on quadrature amplitude modulated (QAM) and phase shift keyed (PSK) constellations, due to the existence of binary mappers which achieve labelling diversity for these modulation schemes.[6,8] The suboptimal binary mappers proposed by Xu et al[8] are used for 64QAM and all PSK constellations. For 16QAM, the mapping structure of Samra et al[6] (illustrated in Figure 1) is used, as it is found to be optimal.[6,8] All constellations are power-normalised such that $\mathcal{E}\{|\Omega_1(l)|^2\} = \mathcal{E}\{|\Omega_2(l)|^2\} = 1$ for all possible labels $l \in [0{:}2^m - 1]$.

The received signal vector, $\mathbf{r}$, during time slot k is thus given by

$$\mathbf{r}_k = \sqrt{\frac{\gamma}{N_t}}\mathbf{H}_k[\Omega_k(\mathbf{L})] + \mathbf{n}_k, \quad k \in [1{:}2], \tag{1}$$

where γ represents the total average signal-to-noise ratio (SNR) of the transmission, assumed to be equally distributed among the N_t transmit antennas. $\mathbf{n}_k = \left[n_{1_k} \ \cdots n_{N_{rk}}\right]^{\mathrm{T}}$ represents additive white Gaussian noise (AWGN) during time slot k, which follows a complex normal distribution with zero mean and unit variance. $\mathbf{H}_k = \left[\mathbf{h}_k^{(1)} \ \cdots \mathbf{h}_k^{(N_t)}\right]$ represents the correlated fading channels during time slot k, which are assumed to be frequency-flat and may either be fast or quasi-static fading over the duration of the 2 time slots. Each vector $\mathbf{h}_k^{(a)}, a \in [1{:}N_t]$, is a column with N_r entries. It is assumed that the fading follows a Nakagami-q amplitude distribution. The entry of $\mathbf{H}_k$ in column a and row b is denoted $h_{b_k}^{(a)} = \left(h_{b_k}^{(a)}\right)^{\mathrm{I}} + \mathrm{j}\left(h_{b_k}^{(a)}\right)^{\mathrm{Q}}, a \in [1{:}N_r], b \in [1{:}N_t], k = [1{:}2]$. The fading parameter q is the ratio of the standard deviations of the quadrature to in-phase components of each entry in $\mathbf{H}_k$, as stated by Amol and Kaur,[34] and lies in the range $0 \leq q \leq 1$. Romero-Jerez and Lopez-Martinez[35] further indicate that q may also be viewed as an indication of the correlation between $\left(h_{b_k}^{(a)}\right)^{\mathrm{I}}$ and $\left(h_{b_k}^{(a)}\right)^{\mathrm{Q}}$. Each component of the elements in $\mathbf{H}_k$ may be modelled as Gaussian-

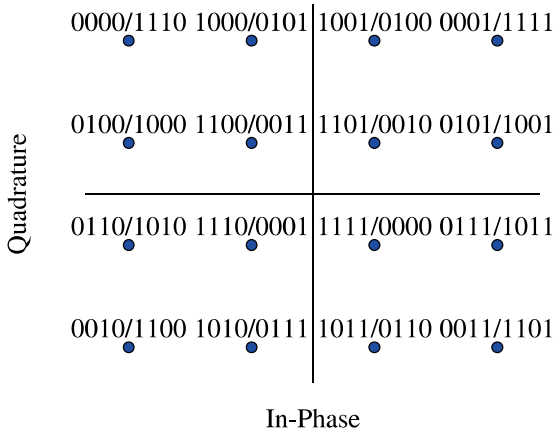

FIGURE 1 16QAM binary constellation mapping. Key: Ω_1/Ω_2

distributed random variables (RVs) such that $\left(h_{b_k}^{(a)}\right)^{\mathrm{I}} \sim \mathcal{N}\left(0, \frac{1}{1+q^2}\right)$ and $\left(h_{b_k}^{(a)}\right)^{\mathrm{Q}} \sim \mathcal{N}\left(0, \frac{q^2}{1+q^2}\right)$ for all $a \in [1{:}N_r]$, $b \in [1{:}N_t]$,$k = [1{:}2]$.[38] The probability density function (PDF) for the Nakagami-q fading amplitude, x, which has zero mean and unit variance is[12]

$$f_x(x) = \frac{x(1+q^2)}{q} \exp\left(-\frac{x^2(1+q^2)^2}{4q^2}\right) I_0\left(\frac{x^2(1-q^4)}{4q^2}\right). \tag{2}$$

It may be observed that the bounds of q correspond to the respective cases of single-sided Gaussian (SSG) ($q = 0$) and Rayleigh ($q = 1$) amplitude distributions.[12] Additionally, in (1), $\mathbf{n}_k$ and $\mathbf{H}_k$ are assumed to have uniform phase distribution.

2.2 | Correlation model

In this paper, the Kronecker correlation model[25] is adopted to relate the correlated channel matrix in the kth time slot ($\mathbf{H}_k$) to an uncorrelated channel matrix in the same time slot ($\breve{\mathbf{H}}_k$), as given in (3).

$$\mathbf{H}_k = \mathbf{C}_r^{\frac{1}{2}} \breve{\mathbf{H}}_k \left(\mathbf{C}_t^{\frac{1}{2}}\right)^{\mathrm{T}}, \quad k \in [1{:}2], \tag{3}$$

where $\mathbf{C}_t$ and $\mathbf{C}_r$ represent the respective antenna correlation matrices at the transmitter and receiver. The $N_r \times N_r$ receive antenna correlation matrix is described by[20]

$$\mathbf{C}_r = \begin{bmatrix} 1 & \rho_r^{(1,2)} & \cdots & \rho_r^{(1,N_r)} \\ \rho_r^{(2,1)} & 1 & \cdots & \rho_r^{(2,N_r)} \\ \vdots & \vdots & \ddots & \vdots \\ \rho_r^{(N_r,1)} & \cdots & \rho_r^{(N_r,N_r-1)} & 1 \end{bmatrix}, \tag{4}$$

where $\rho_r^{(i,j)}$ denotes the correlation coefficient between the ith and jth receive antennas. $N_t \times N_t$ matrix $\mathbf{C}_t$ is similarly defined in terms of the correlation coefficients between the ith and jth transmit antennas, $\rho_t^{(i,j)}$. Both $\mathbf{C}_t$ and $\mathbf{C}_r$ are symmetrical matrices such that $\rho_t^{(i,j)} = \rho_t{}^{(j,i)}; i \neq j, i, j \in [1{:}N_t]$ and $\rho_r^{(i,j)} = \rho_r{}^{(j,i)}; i \neq j, i, j \in [1{:}N_r]$. It is noted that instances of complex correlation coefficients exist in literature, in which case $\rho_t^{(i,j)} = \bar{\rho}_t{}^{(j,i)}; i \neq j, i, j \in [1{:}N_t]$ and $\rho_r^{(i,j)} = \bar{\rho}_r{}^{(j,i)}; i \neq j, i, j \in [1{:}N_r]$, where $\bar{(\cdot)}$ denotes the complex conjugate. However, in the context of only spatial correlation, only the magnitude of the correlation coefficient is of interest. Hence, this work only considers real values of ρ_t and ρ_r.

It is shown in other studies[19-21] that the correlation coefficient between the ith and jth antennas in a linear array is given by

$$\rho^{(i,j)} = J_0\left(\frac{2\pi}{\lambda} \mu^{(i,j)}\right). \tag{5}$$

Based on (5), for receive antennas with uniformly distributed angle of arrival, the correlation coefficient $\rho_r^{(i,j)}$ is expressed in terms of receive antenna spacing $\mu_r^{(i,j)}$. Similarly, for transmit antennas with uniformly distributed angle of transmission, $\rho_t^{(i,j)}$ is expressed in terms of $\mu_t^{(i,j)}$.

If antennas are not arranged linearly, alternate models to represent the correlation between antennas must be used. Examples of such cases are when antennas are very closely spaced, which results in a constant correlation between all antennas.[39,40] If they are arranged nonlinearly, such that they are all equispaced in some sense, correlation between antennas may be described by the exponential correlation model.[39,41,42]

2.3 | Detection

Maximum-likelihood detection (MLD), assuming perfect channel state information, is used to estimate the transmitted information label vector $\tilde{\mathbf{L}}$ according to (6).

$$\tilde{\mathbf{L}} = \underset{\hat{\mathbf{L}}\in\boldsymbol{\xi}}{\arg\min} \sum_{k=1}^{2} \left\| \mathbf{r}_k - \sqrt{\frac{\gamma}{N_t}} \mathbf{H}_k[\Omega_k(\hat{\mathbf{L}})] \right\|^2, \tag{6}$$

where $\boldsymbol{\xi}$ is the set of all 2^{mN_t} possible transmitted label vectors and $\hat{\mathbf{L}}$ is a candidate label vector from $\boldsymbol{\xi}$.

3 | ERROR PERFORMANCE ANALYSIS

The union bound of the average bit error probability (ABEP) for an $N_t \times N_r$ USTLD system has previously been derived under the assumption that only one received label is detected erroneously in the high SNR region.[8,14] While the results presented in previous works on USTLD systems[8,14] validate this assumption, it cannot be used when the methods of correlation analysis developed by Hedayet et al[18] are applied. For this reason, this paper first derives the ABEP under uncorrelated conditions for a Nakagami-q fading channel using the same assumption as previous works.[8,14] Thereafter, the analysis is extended to the correlated case without this assumption. The expressions derived are valid for both fast fading and quasi-static fading.

3.1 | Uncorrelated Nakagami-q error performance

When evaluating the uncorrelated ABEP of $N_t \times N_r$ USTLD systems, the assumption that only one received label is detected erroneously in the high SNR region may be used.[8,14]

From Patel et al,[14] the union bound of the ABEP is given by

$$P_b(\gamma) \leq \sum_{L=0}^{2^m-1} P(L) \sum_{\substack{\tilde{L}=0 \\ \tilde{L}\neq L}}^{2^m-1} \frac{\delta(L,\tilde{L})}{m} P\left(L \to \tilde{L}\right). \tag{7}$$

In (7), $P(L) = 2^{-m}$ is the uniformly distributed probability of label L being transmitted. $\delta(L,\tilde{L})$ and $P\left(L \to \tilde{L}\right)$ are, respectively, the number of bit errors and the pairwise error probability (PEP) between L and estimated label $\tilde{L}$.

Given the assumption that only one symbol pair is incorrect, the conditional PEP (8) may be expressed in terms of the Gaussian Q-function ,[43] $Q(x) = \frac{1}{\pi}\int_0^{\frac{\pi}{2}} \exp\left(\frac{x}{2\sin^2(y)}\right) \mathrm{d}y$, and 4 chi-squared RVs, ϕ_l,ϕ_2,ϕ_3, and ϕ_4 as follows:

$$\begin{aligned} &P\left(\mathbf{L} \to \tilde{\mathbf{L}} | \mathbf{H}_1, \mathbf{H}_2\right) \\ &= P\left(\sum_{k=1}^{2} \left\| \mathbf{r}_k - \sqrt{\frac{\gamma}{N_t}} \mathbf{H}_k[\Omega_k(\tilde{\mathbf{L}})] \right\|^2 < \sum_{k=1}^{2} \|\mathbf{n}_k\|^2 \right) \end{aligned} \tag{8}$$

$$= Q\left(\sqrt{\phi_1 + \phi_2 + \phi_3 + \phi_4}\right). \tag{9}$$

Following the procedure given in the appendix of Xu et al,[8] it may be shown that in a Nakagami-q distribution, the chi-squared RVs are formed from Gaussian-distributed RVs with zero mean and different variances related by the fading parameter q.[35] Each of the chi-squared RVs has N_r degrees of freedom and may be defined by

$$\phi_l = \sum_{p=1}^{N_r} \alpha_{p_l}^2, \quad l \in [1{:}4]. \tag{10}$$

The Gaussian RVs α_{p_l} follow normal distributions (as derived in the appendix, Section A) such that

$$\alpha_{p_1} \sim \mathcal{N}\left(0, \frac{\gamma \left| d_1(L,\tilde{L}) \right|^2}{2N_t(1+q^2)}\right) \tag{11}$$

$$\alpha_{p_2} \sim \mathcal{N}\left(0, \frac{\gamma q^2 \left|d_1(L,\tilde{L})\right|^2}{2N_t(1+q^2)}\right) \tag{12}$$

$$\alpha_{p_3} \sim \mathcal{N}\left(0, \frac{\gamma \left|d_2(L,\tilde{L})\right|^2}{2N_t(1+q^2)}\right) \tag{13}$$

$$\alpha_{p_4} \sim \mathcal{N}\left(0, \frac{\gamma q^2 \left|d_2(L,\tilde{L})\right|^2}{2N_t(1+q^2)}\right), \tag{14}$$

where $d_k(L,\tilde{L})$, $k \in [1{:}2]$ is the difference between the symbols obtained by mapping L and $\tilde{L}$ using mapper Ω_k, as shown in (15).

$$d_k(L,\tilde{L}) = \Omega_k(L) - \Omega_k(\tilde{L}), \quad k \in [1{:}2] \tag{15}$$

As in Xu et al,[8] the final unconditional PEP is obtained by integrating (9) over the PDF of the underlying chi-squared RVs. Applying the trapezoidal approximation to this integral, as done in previous works[8,14] produces the result

$$P(L \to \tilde{L}) \approx \frac{1}{4n} \prod_{k=1}^{2} \left[\mathcal{M}_k\left(\frac{1}{2}, \left|d_k(L,\tilde{L})\right|^2\right)\right]^{N_r} + \frac{1}{2n} \sum_{m=1}^{n-1} \prod_{k=1}^{2} \left[\mathcal{M}_k\left(\frac{1}{2\sin^2\left(\frac{m\pi}{2n}\right)}, \left|d_k(L,\tilde{L})\right|^2\right)\right]^{N_r}. \tag{16}$$

In (16), n is an arbitrarily large integer that allows the trapezoidal approximation to converge to the integral result. $\mathcal{M}_k(s,x)$ denotes the moment generating function (MGF) of the received signal amplitude during the kth time slot ($k \in [1{:}2]$), as a function of dummy variables s and x. For a Nakagami-q distribution, the MGF is given by[12]

$$\mathcal{M}_k(s,x) = \left[1 + \frac{s\gamma x}{N_t} + \left(\frac{sq\gamma x}{N_t(1+q^2)}\right)^2\right]^{-\frac{1}{2}}. \tag{17}$$

3.2 | Correlated Nakagami-q error performance

To apply the method of correlated channel analysis used given in Hedayet et al,[18] the union bound of the USTLD system considered is obtained by considering all possible combinations of transmitted and detected label vectors. The union bound is then modified from (7) to reflect that it is now dependent on the transmitted label vector $\mathbf{L}$ and the estimated label vector $\tilde{\mathbf{L}}$. The bound is given by

$$P_b(\gamma) \leq \sum_{\mathbf{L} \in \boldsymbol{\xi}} P(\mathbf{L}) \sum_{\substack{\tilde{\mathbf{L}} \in \boldsymbol{\xi} \\ \mathbf{L} \neq \tilde{\mathbf{L}}}} \frac{\delta(\mathbf{L}, \tilde{\mathbf{L}})}{mN_t} P\left(\mathbf{L} \to \tilde{\mathbf{L}}\right). \tag{18}$$

Note that $\boldsymbol{\xi}$ is the set of all possible transmitted label vectors, as defined in Section 2.3. As in Section 3.1, $\delta(\mathbf{L}, \tilde{\mathbf{L}})$ is the total number of bit errors between $\mathbf{L}$ and $\tilde{\mathbf{L}}$.

In (18), the probability that label vector $\mathbf{L}$ was transmitted, $P(\mathbf{L})$, is uniformly distributed, resulting in

$$P(\mathbf{L}) = 2^{-mN_t}. \tag{19}$$

The PEP, $P\left(\mathbf{L} \to \tilde{\mathbf{L}}\right)$, is defined in terms of label vectors, as opposed to scalar labels used in Section 3.1. The vector of distances between the symbols defined by label vectors $\mathbf{L}$ and $\tilde{\mathbf{L}}$ on mapper Ω_k is given in terms of (15) as follows:

$$\mathbf{d}_k = \begin{bmatrix} d_k(L_1, \tilde{L}_1) \\ \vdots \\ d_k(L_{N_t}, \tilde{L}_{N_t}) \end{bmatrix}, \quad k \in [1{:}2]. \tag{20}$$

The nonzero eigenvalue of $\mathbf{d}\cdot\mathbf{d}^{\mathrm{H}}$ is analogous to the squared Euclidean distance $|d|^2$ of the scalar case.

As shown in (3), the Kronecker correlation model shows that the correlated channel matrix during the kth time slot, $\mathbf{H}_k, k \in [1{:}2]$, may be expressed in terms of an artificial, uncorrelated channel matrix $\breve{\mathbf{H}}_k$. By adopting this model and applying the analysis techniques of Hedayet et al,[18] the ABEP in *correlated* channels is found by using the result found for *uncorrelated* channels and weighting the MGFs (17) in the PEP expression by the N_r eigenvalues of the receive antenna correlation matrix (21). The squared Euclidean distances are replaced by the nonzero eigenvalue of the squared-distance weighted transmit antenna correlation matrix in each time slot (22). It is noted that in (22), $\mathbf{d}_k\cdot\mathbf{d}_k^{\mathrm{H}}\cdot\mathbf{C}_t$ has rank one and thus there is only one nonzero eigenvalue for each value of $k, k \in [1{:}2]$, as shown by Hedayet et al.[18] This would not be the case under the assumption that only one label is detected incorrectly in the high SNR region, as used in Section 3.1, and hence, this assumption is inappropriate for the correlated channel analysis of USTLD systems.

$$\begin{bmatrix} \nu_1 \\ \vdots \\ \nu_{N_r} \end{bmatrix} = \mathcal{V}\{\mathbf{C}_r\} \tag{21}$$

$$\eta_k = \mathcal{V}\{\mathbf{d}_k\cdot\mathbf{d}_k^{\mathrm{H}}\cdot\mathbf{C}_t\}, \quad \eta_k \neq 0, k \in [1{:}2] \tag{22}$$

The final result for the PEP of an $N_t \times N_r$ USTLD system in correlated Nakagami-q channels is thus

$$P\left(\mathbf{L}\to\tilde{\mathbf{L}}\right) \approx \frac{1}{4n}\prod_{k=1}^{2}\prod_{j=1}^{N_r}\mathcal{M}_k\left(\frac{1}{2}, \nu_j\eta_k\right) + \frac{1}{2n}\sum_{m=1}^{n-1}\prod_{k=1}^{2}\prod_{j=1}^{N_r}\mathcal{M}_k\left(\frac{1}{2\sin^2\left(\frac{m\pi}{2n}\right)}, \nu_j\eta_k\right). \tag{23}$$

The result for correlated PEP (23) is of a similar form to that of the uncorrelated PEP (16). The difference between these 2 expressions is that the second argument of MGF $\mathcal{M}_k$ is the squared Euclidean distance $\left|d_k(L, \tilde{L})\right|^2$ for the uncorrelated PEP, whereas it is the eigenvalue product $\nu_j\eta_k$ for the correlated PEP.

It may be noted that uncorrelated USTLD systems may also be analysed using this approach. In the case of no transmit antenna correlation, the matrix $\mathbf{C}_t$ is an $N_t \times N_t$ identity matrix. Similarly, for no receive antenna correlation, $\mathbf{C}_r$ is an $N_r \times N_r$ identity matrix.

4 | RESULTS AND DISCUSSION

In this section, results are presented to investigate the effects of spatial correlation on $N_t \times N_r$ USTLD systems in Nakagami-q fading. The first set of results, given in Figure 2, verifies that the theoretical bound of the ABEP for correlated $N_t \times N_r$ USTLD systems in the presence of Nakagami-q fading (derived in Section 3) converges to simulated results. Thereafter, the change in error performance as a result of fading parameter q is demonstrated in Figure 3. USTLD systems are then studied under transmit and receive correlation independently to determine which causes greater degradation of error performance, and the results are given in Figure 4. Finally, a comparison between USTLD and conventional MIMO STBC Alamouti[13] systems is presented in Figure 5, wherein the susceptibility of each system to antenna correlation is determined. For all results produced, antennas are equidistantly spaced and arranged linearly at both the transmitter and the receiver (that is, $\mu_t^{(i,i+1)} = \mu_t^{(1,2)} = \mu_t$, $i \in [1{:}N_t - 1]$ and $\mu_r^{(j,j+1)} = \mu_r^{(1,2)} = \mu_r$, $j \in [1{:}N_r - 1]$) and the correlation between them is determined by (5).

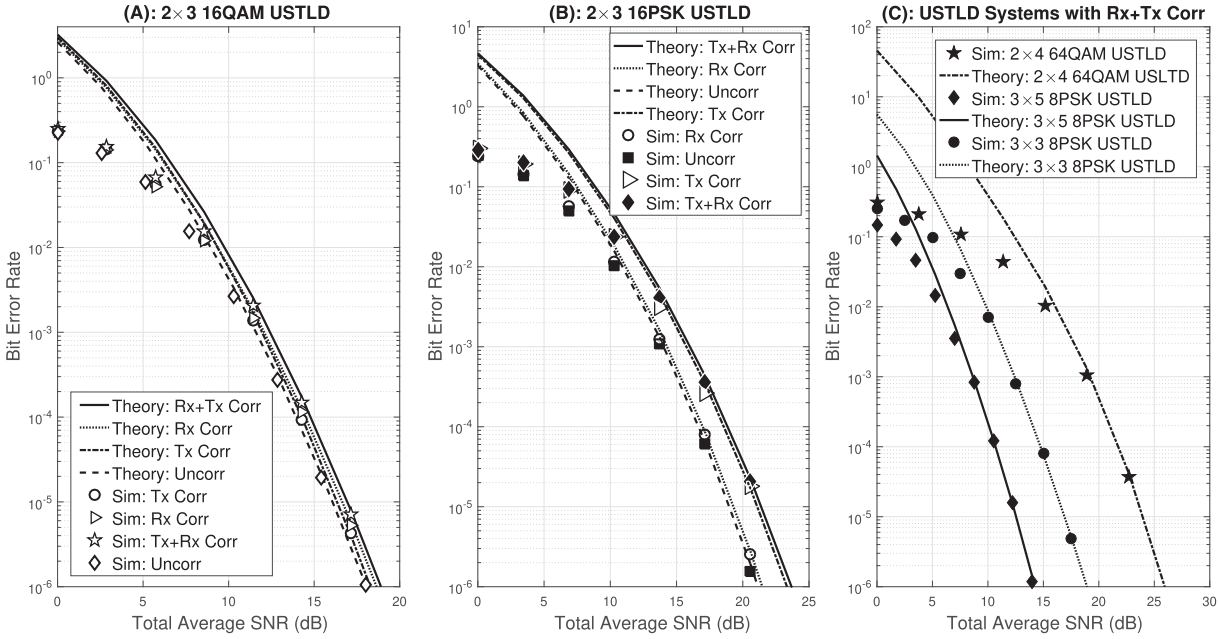

FIGURE 2 Comparison of theoretical and simulated results. SNR, signal-to-noise ratio; USTLD, Uncoded Space Time Labelling Diversity

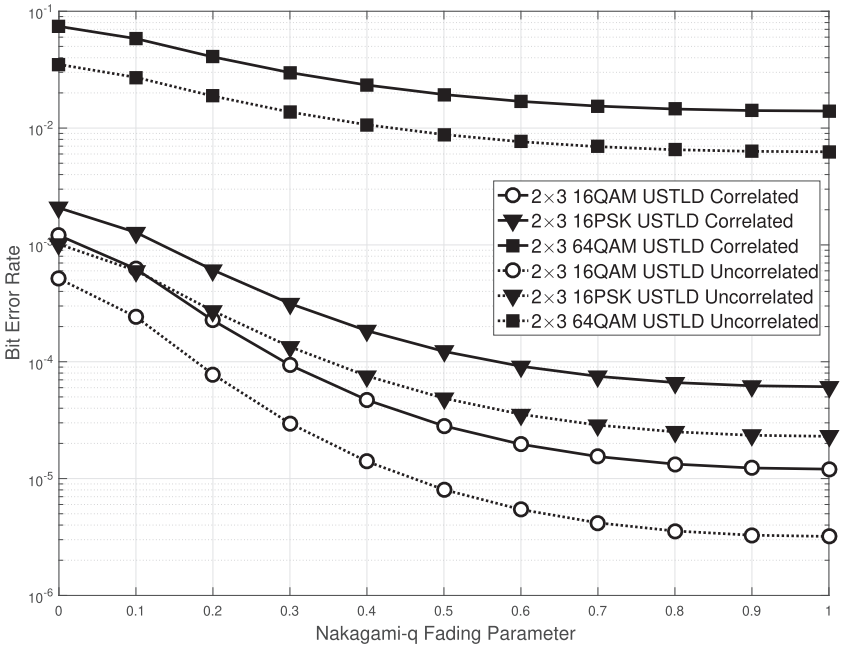

FIGURE 3 Effect of fading parameter q at 20dB. USTLD, Uncoded Space Time Labelling Diversity

In Figure 2A,B, simulations are shown for 16QAM and 16PSK USTLD systems under the conditions of (1) both transmit and receive antenna correlation, (2) only transmit antenna correlation, (3) only receive antenna correlation, and (4) uncorrelated transmit and receive antennas. To show that the ABEP is valid for other modulation orders and antenna array sizes, results are also shown for 2×4 64QAM, 3×3 8PSK, and $3\times$ 5 8PSK USTLD systems with both transmit and receive antenna correlation (Figure 2C). The results show that the bound of the ABEP converge to Monte Carlo simulation output in the high SNR region for all systems presented. The transmit antenna spacing (μ_t), receive antenna spacing (μ_r), and fading parameter (q) used for each system are presented in Table 1.

Figure 3 shows the change in error performance of both correlated and uncorrelated USTLD systems across the range of the Nakagami-q fading parameter. The correlated results were produced using arbitrary transmit and receive correlation parameters $\mu_t = 0.21\lambda$ and $\mu_r = 0.30\lambda$. The results indicate that the error performance of USTLD in the presence of SSG fading $(q = 0)$ is significantly worse than in Rayleigh fading $(q = 1)$. In particular, 16QAM USTLD in SSG

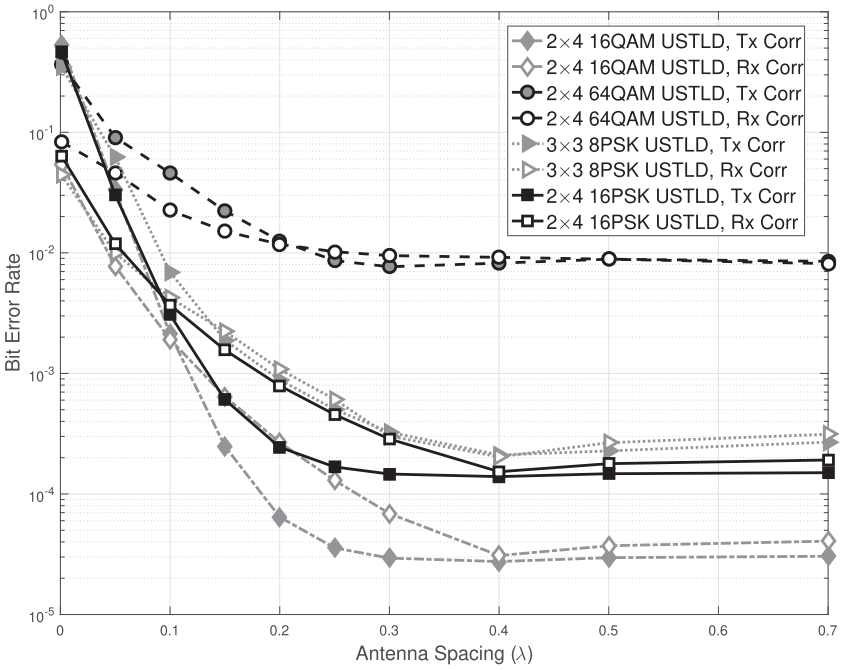

FIGURE 4 Comparing the effects of transmit and receive antenna correlation at 15dB ($q = 0.2$). USTLD, Uncoded Space Time Labelling Diversity

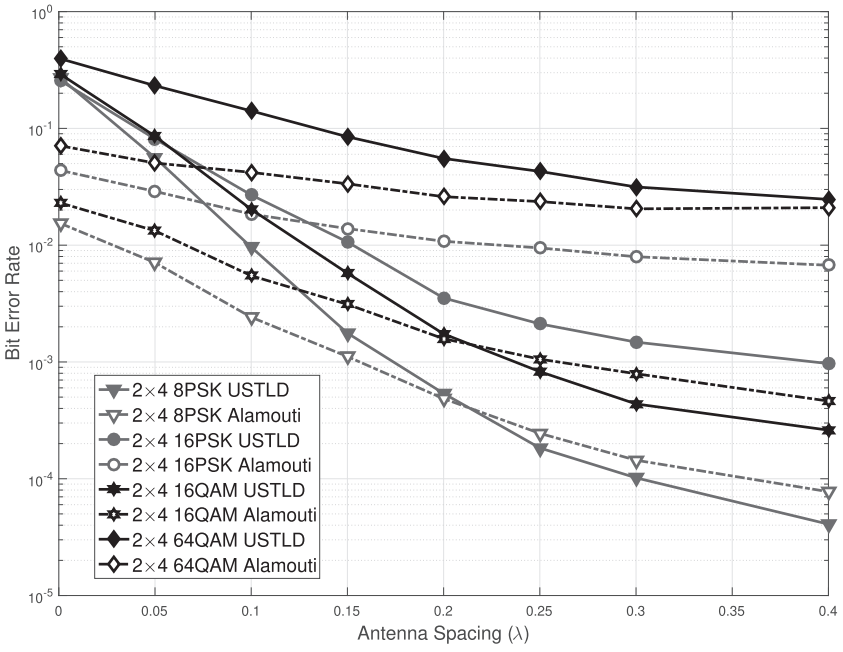

FIGURE 5 Comparing the performance of USTLD and Alamouti-coded systems at 13dB ($q = 0.7$). USTLD, Uncoded Space Time Labelling Diversity

TABLE 1 Simulation parameters for Figure 2

Modulation	μ_t	μ_r	q
16PSK	0.15λ	0.70λ	0.4
16QAM	0.24λ	0.30λ	0.8
8PSK	0.25λ	0.75λ	0.9
64QAM	0.24λ	0.5λ	0.3

fading is 2 orders of magnitude worse than in Rayleigh fading. Similarly, 16PSK USTLD degrades by an order of magnitude. It is also observed that the performance is approximately constant in the range $0.6 \leq q \leq 1$. Finally, it is noted the results for correlated and uncorrelated systems follow the same trend. This may be attributed to the in-phase and

quadrature components of the fading having different variances, as specified in Section 2.1 For smaller values of q, the power of the quadrature component is almost negligible. Hence, the power of the in-phase component dominates the total power of the fading coefficient. As q increases above 0.6, the powers of the in-phase and quadrature components become comparable; hence, further increases in q have a smaller effect on error performance.

The next set of results investigates the degradation in error performance of USTLD systems due to antenna correlation, by considering transmit and receive antenna correlation independently. The results are presented in Figure 4 for 3×3 8PSK, 2×4 16PSK, 2×4 16QAM, and 2×4 64QAM USTLD systems at an SNR of $\gamma=15$dB with arbitrary Nakagami-q fading parameter $q=0.2$.

Intuitively, as the spacing between antennas increase, the correlation between them decreases. This may be confirmed numerically by (5). As such, the gradient of the curves in Figure 4 indicates the rate at which error performance improves as antenna correlation decreases. By observing the gradient of the curves in the range $0<\mu\leq0.4\lambda$, it is found that transmit antenna correlation causes a more severe degradation in error performance than receive antenna correlation in USTLD systems. This concurs with the results shown in Figure 2A,B, where it is observed that there is a larger dB gap between the uncorrelated and transmit antenna correlated systems than between the uncorrelated and receive antenna correlated systems. The reason for transmit antenna correlation having a more dominant effect on performance may be explained mathematically. From (22), it is observed that the transmit antenna correlation matrix $\mathbf{C}_t$ is weighted by the distance vector product $\mathbf{d}\cdot\mathbf{d}^{\mathrm{H}}$ before being decomposed into its eigenvalues. By contrast, $\mathbf{C}_r$ undergoes eigenvalue decomposition directly, as shown in (21). Thus, the eigenvalue product that governs the PEP of correlated USTLD systems (shown in (23)) is more affected by the transmit antenna correlation matrix. A secondary observation is that all curves have a very flat gradient in the region $\mu>0.4\lambda$. This indicates that spacing antennas further than 0.4λ apart does not significantly improve the robustness of USTLD systems to antenna correlation. Hence, 0.4λ is a theoretical optimal spacing for a linear array of antennas used for USTLD systems, which balances correlation and small form factor.

These results provide a guideline for implementing USTLD systems: to reduce degradation in error performance due to spatial correlation, it is more important to avoid correlation between transmit antennas than receive antennas. This may be achieved by ensuring that transmit antennas are spaced further than 0.4λ apart.

The final set of results investigates the susceptibility of USTLD systems to spatial correlation when compared with existing MIMO systems. To provide a fair comparison in terms of both spectral efficiency and antenna array sizes, the USTLD systems are compared with traditional Alamouti STBC systems.[13] Thus, the systems investigated in Figure 5, and the curves associated with it, are constrained to only $N_t=2$ transmit antennas. The results compare 2×4 systems with both transmit and receive antenna correlation at SNR $\gamma=13$dB and with Nakagami-q fading parameter $q=0.7$. The spacing between all antennas at both the transmitter and the receiver are assumed equal (ie, $\mu_t^{(i,i+1)}=\mu_r^{(j,j+1)}=\mu$, $i\in[1{:}N_t-1]$,$j\in[1{:}N_r-1]$). From the findings of Figure 4, it is only necessary to consider antenna spacings in the range $0<\mu\leq0.4\lambda$, as greater spacings have negligible impact on performance.

The results in Figure 5 show that the error performance of USTLD systems at high antenna correlation worse than that of Alamouti STBC systems. This may be observed in the regions $0<\mu\leq0.2\lambda$ for the 8PSK and 16QAM systems, $0<\mu\leq0.13\lambda$ for 16PSK, and across the full range $0<\mu\leq0.4\lambda$ for 64QAM. This indicates that at high antenna correlations, labelling diversity decreases the error performance of MIMO systems compared with existing systems. Furthermore, USTLD systems are found to be more susceptible to antenna correlation as all curves show steeper gradients than the comparable Alamouti systems. This is in agreement with the results of previous work,[24] wherein dual-correlated USTLD systems are found to be more susceptible to antenna correlation than comparable conventional MIMO systems.

5 | CONCLUSION

This paper presents an analysis of the performance of USTLD in the presence of spatial correlation. An expression for the union bound of the ABEP is derived for the case of the Nakagami-q fading model in both correlated and uncorrelated channels. This expression is verified by the results of Monte Carlo simulations, which show convergence in the high SNR region. The results presented also show the effect of the Nakagami-q fading parameter on error performance: as the fading parameter decreases, so does error performance. In particular, the 16-ary modulation schemes show performance degradation of 2 orders of magnitude.

It is further concluded that transmit antenna correlation has a greater impact on degrading the error performance of USTLD systems than receive antenna correlation. Results indicate that, for linear antenna arrangements, there is a

threshold spacing of 0.4λ, after which greater antenna spacings do not improve the robustness towards spatial correlation. This provides a valuable practical guideline for implementing USTLD systems. Future work may consider determining the optimal antenna spacings of USTLD systems with nonlinear antenna configurations.

Finally, it is found that 2×4 USTLD systems are more susceptible to spatial correlation than comparable MIMO Alamouti STBC systems. It is found that labelling diversity decreases the error performance of MIMO systems at high antenna correlations when compared with the existing Alamouti STBC system. Another open problem for future work is to study the effects of correlation on the capacity of USTLD systems.

ACKNOWLEDGEMENTS

Thank you to Dr Peter Akuon of the University of Nairobi for offering his assistance in modelling transmit antenna correlation.

ORCID

Sulaiman Saleem Patel http://orcid.org/0000-0003-3557-3645
Tahmid Quazi http://orcid.org/0000-0002-1288-4224

REFERENCES

1. Huang Y, Ritcey JA. Improved 16-QAM constellation labeling for BI-STCM-ID with the Alamouti scheme. *IEEE Commun Letters*. 2005;9(2):157-159.
2. Huang Y, Ritcey JA. Optimal constellation labeling for iteratively decoded bit-interleaved space-time coded modulation. *IEEE Trans Inf Theory*. 2005;51(5):1865-1871.
3. Krasicki M. Improved labelling diversity for iteratively-decoded multiantenna systems. In: Proc. 7th Int. Conf. on Wireless Commun. and Mobile Computing(IWCMC), Istanbul (Turkey); 2011:359-364.
4. Krasicki M.. Essence of 16-QAM labelling diversity. *IET Electronics Lett*. 2013;49(8):567-569.
5. Seddik KG, Ibrahim AS, Liu KJR. Trans-modulation in wireless relay networks. *IEEE Commun Lett*. 2008;12(3):170-172.
6. Samra H, Ding Z, Hahn P. Symbol mapping diversity design for multiple packet transmissions. *IEEE Trans Commun*. 2005;53(5):810-817.
7. Zhao Z, Zhou L, Zheng X, Park S-E. Enhanced constellation rearrangement for HARQ with symbol combining. In: IEEE Mobile WiMax Symp. (MWS). Napa Valley, CA(USA); 2009. https://doi.org/10.1109/MWS.2009.21.
8. Xu H, Govindasamy K, Pillay N. Uncoded space-time labeling diversity. *IEEE Commun Lett*. 2016;20(8):1511-1514.
9. Govindasamy K, Xu H, Pillay N. Space-time block coded spatial modulation with labeling diversity. *Int J Commun Syst*. 2017:e3395. https://doi.org/10.1002/dac.3395
10. Pillay N, Xu H. *IEEE Commun Lett*. 2017. https://doi.org/10.1109/LCOMM.2017.2770145
11. Goldsmith A. *Wireless Communications*. Cambridge (USA): Cambridge University Press; 2005.
12. Simon MK, Alouini M-S. *Digital Communication Over Fading a Unified Approach to Performance Analysis*. New York (USA): John Wiley & Sons Inc.; 2000.
13. Alamouti SM. Simple transmit diversity technique for wireless communications. *IEEE J on Sel Areas in Commun*. 1998;16(8):1451-1458.
14. Patel SS, Quazi T, Xu H. Full MIMO Uncoded Space Time Labeling Diversity with Low Complexity Detection. IET Commun. 2017; under review.
15. Tseng S-M, Liao C-Y.. Distributed orthogonal and quasi-orthogonal space-time block code with embedded AAF/DAF matrix elements in wireless relay networks with four relays. *Wirel Pers Commun*. 2014;75(2):1187-1198.
16. Choi M, Lee H, Nam H. Exact and asymptotic PEP derivations for various quasi-orthogonal space-time block codes. *Electronics Lett*. 2013;49(21):1358-1360.
17. Ranju MAAA, Rafi RS. Analysis of rate one quasi-orthogonal space-time block coding over Rayleigh fading channel. *Int J Commun Netw and Syst Sci*. 2014;7:196-202.
18. Hedayet A, Shah H, Nosratinia A. Analysis of space-time coding in correlated fading channels. *IEEE Trans on Wirel Commun*. 2005;4(6):2882-2891.
19. Stüber GL. *Principles of Mobile Communication*. New York (USA): Kluwer Academic Publishers; 2002.
20. Akoun PO, Xu H. Optimal error analysis of receive diversity schemes on arbitrarily correlated Rayleigh fading channels. *IET Commun*. 2016;10(7):854-861.

21. Ebrahimi-Tofighi N, Ardebilipour M, Shahabadi M. Receive and transmit array antenna spacing and their effect on the performance of SIMO and MIMO systems by using an RCS channel model. *Int J of Elec Comp Energetic Electronic and Commun Eng*. 2007;1(12):1732-1736.
22. Rappaport TS, Sun S, Mayzus R, et al.. Millimeter wave mobile communications for 5G cellular: it will work!. *IEEE Access*. 2013;1:335-349.
23. Fang L, Bi G, Cot AC. New method of performance analysis for diversity reception with correlated Rayleigh-fading signals. *IEEE Trans on Vehicular Tech*. 2000;49(5):1807-1812.
24. Patel SS, Quazi T, Xu H. Performance of uncoded space-time labeling diversity in dual-correlated Rayleigh-fading channels. In: Proc. Southern Africa Telecommunication Networks and Applications Conference (SATNAC), Freedom of the Seas Cruise Liner, Barcelona (Spain); 2017:68-73.
25. Kermoal JP, Schumacher L, Pedersen KI, Mogensen PE, Frederiksen F. A stochastic MIMO radio channel model with experimental validation. *IEEE J on Sel Areas in Commun*. 2002;20(6):1211-1226.
26. Khumbani B, Mohandas VK, Singh RP, Kabra S, Kshetrimayum RS. Analysis of space-time block coded spatial modulation in correlated Rayleigh and Rician fading channels. In: IEEE Conf. on DSP, Singapore (Singapore); 2015:516-520.
27. Varshney N, Goel A, Jagannatham AK. Cooperative communication in spatially modulated MIMO systems. In: IEEE Wireless Commun. and Networking Conf WCNC, Doha (Qatar):2016.
28. Weichselberger W, Herdin M, Ozcelik H, Bonek E. A stochastic MIMO channel model with join correlation of both link ends. *IEEE Trans on Wirel Communic*. 2006;5(1):90-100.
29. Tulino AM, Lozano A, Verdú S. Impact of antenna correlation on the capacity of multiantenna channels. *IEEE Trans on Inf Theory*. 2005;51(7):2491-2509.
30. Lin C, Veeravalli VV. Optimal linear dispersion codes for correlated MIMO channels. *IEEE Trans Wirel Commun*. 2008;7(2):657-666.
31. Raghavan V, Sayeed AM, Veeravalli VV. Semiunitary precoding for spatially correlated MIMO channels. *IEEE Trans on Inf Theory*. 2011;57(3):1284-1298.
32. Lin C, Raghavan V, Veeravalli VV. To code or not to code across time: space-time coding with feedback. *IEEE J on Sel Areas in Commun*. 2008;26(8):1588-1598.
33. Moustakas A, Baranger H, Balents L, Sengupta A, Simon S. Communication through a diffusive medium: coherence and capacity. *Sci*. 2000;287:287-290.
34. Amol R, Kaur K. Performance analysis of Hoyt fading channel for M-ary and Monte Carlo simulation. *Int J of Adv Comput Manag Stud*. 2016;1(3):13-19.
35. Romero-Jerez JM, Lopez-Martinez FJ. A new framework for the performance analysis of wireless communications under Hoyt (Nakagami-q) hading. *IEEE Trans Inf Theory*. 2017;63(3):1693-1702.
36. Chytil B.. The distribution of amplitude scintillation and te conversion of scintillation indices. *J of Atmos Terr Phys*. 1967;29(9):1175-1177.
37. Weisstein EW. Modified Bessel Function of the First Kind (A Wolfram Web Resource). [Online] Cited 2017-11-11. Available at: http://mathworld.wolfram.com/ModifiedBesselFunctionofheFirstKind.html
38. Ropokis GA, Rontogiannis AA, Mathiopoulos PT. Quadratic Forms in Normal RVs: theory and applications to OSTBC over Hoyt Fading Channels. *IEEE Trans Wirel Commun*. 2008;7(12):5009-5019.
39. Aalo VA. Performance of maximal-ratio diversity systems in a correlated Nakagami-fading environment. *IEEE Trans Commun*. 1995;43(8):2360-2369.
40. Vaughan RG, Anderson JB. Antenna diversity in mobile communications. *IEEE Trans Veh Technol*. 1987;36(4):149-172.
41. Albdran S, Alshammari A, Matin MA. Spectral and energy efficiency for massive MIMO systems using exponential correlation model. In: IEEE 7th Annual Comp. and Commun. Workshop and Conf. (CCWC), Las Vegas, NV (USA):2017.
42. Loyka SL. Channel capacity of MIMO architecture using the exponential correlation matrix. *IEEE Commun Lett*. 2001;5(9):369-371.
43. Craig JW. A new, simple, and exact result for calculating the probability of error for two-dimensional signal constellations. In: IEEE Military Commun. Conf. (MILCOM), McLean, VA (USA); 1991:571-575.

How to cite this article: Patel S S, Quazi T, Xu H. Error performance of Uncoded Space Time Labelling Diversity in spatially correlated Nakagami-q channels. *Int J Commun Syst*. 2018;31:e3720. https://doi.org/10.1002/dac.3720

APPENDIX A

DETAILS OF UNCORRELATED NAKAGAMI-Q DERIVATION

To show that the PEP may be expressed in terms of 4 chi-squared RVs, as stated in Section 3.1, the inequality for the conditional PEP (8) is first modified to produce (A1). The notation used assumes without loss of generality that the label $L_i, i \in [1{:}N_t]$, was detected erroneously. Thus, $\mathbf{H}_k\left([\Omega_k(\mathbf{L})]-[\Omega_k(\tilde{\mathbf{L}})]\right) = \mathbf{h}_k^{(i)}\left(\Omega_k(L_i)-\Omega_k(\tilde{L}_i)\right) = \mathbf{h}_k^{(i)} d_k$, where the abridged notation $d_k = d_k(L_i, \tilde{L}_i)$ and $d_k(L, \tilde{L})$ is given in (15).

$$P\left(\mathbf{L}\rightarrow\tilde{\mathbf{L}}|\mathbf{H}_1,\mathbf{H}_2\right) = P\left(\sum_{k=1}^{2}\left\|\sqrt{\frac{\gamma}{N_t}}\mathbf{h}_k^{(i)} d_k + \mathbf{n}_k\right\|^2 < \sum_{k=1}^{2}\|\mathbf{n}_k\|^2\right) \tag{A1}$$

The summed terms on the lesser side of the inequality may be written in terms of in-phase and quadrature components as follows:

$$\begin{aligned}
&\sum_{k=1}^{2}\left\|\sqrt{\frac{\gamma}{N_t}}\mathbf{h}_k^{(i)} d_k + \mathbf{n}_k\right\|^2 \\
&= \sum_{k=1}^{2}\left\|\left(\sqrt{\frac{\gamma}{N_t}}\left(\mathbf{h}_k^{(i)}\right)^{\mathrm{I}} d_k^{\mathrm{I}} - \sqrt{\frac{\gamma}{N_t}}\left(\mathbf{h}_k^{(i)}\right)^{\mathrm{Q}} d_k^{\mathrm{Q}} + \mathbf{n}_k^{\mathrm{I}}\right) + \mathrm{j}\left(\sqrt{\frac{\gamma}{N_t}}\left(\mathbf{h}_k^{(i)}\right)^{\mathrm{I}} d_k^{\mathrm{Q}} + \sqrt{\frac{\gamma}{N_t}}\left(\mathbf{h}_k^{(i)}\right)^{\mathrm{Q}} d_k^{\mathrm{I}} + \mathbf{n}_k^{\mathrm{Q}}\right)\right\|^2 \\
&= \sum_{k=1}^{2}\sum_{p=1}^{N_r}\left[\left(\sqrt{\frac{\gamma}{N_t}}\left(h_{p_k}^{(i)}\right)^{\mathrm{I}} d_k^{\mathrm{I}} - \sqrt{\frac{\gamma}{N_t}}\left(h_{p_k}^{(i)}\right)^{\mathrm{Q}} d_k^{\mathrm{Q}} + n_{p_k}^{\mathrm{I}}\right)^2 + \left(\sqrt{\frac{\gamma}{N_t}}\left(h_{p_k}^{(i)}\right)^{\mathrm{I}} d_k^{\mathrm{Q}} + \sqrt{\frac{\gamma}{N_t}}\left(h_{p_k}^{(i)}\right)^{\mathrm{Q}} d_k^{\mathrm{I}} + n_{p_k}^{\mathrm{Q}}\right)^2\right] \\
&= \sum_{k=1}^{2}\sum_{p=1}^{N_r}\left[\left(\sqrt{\frac{\gamma}{N_t}}\left(h_{p_k}^{(i)}\right)^{\mathrm{I}} d_k^{\mathrm{I}}\right)^2 + \left(\sqrt{\frac{\gamma}{N_t}}\left(h_{p_k}^{(i)}\right)^{\mathrm{Q}} d_k^{\mathrm{Q}}\right)^2 + \left(\sqrt{\frac{\gamma}{N_t}}\left(h_{p_k}^{(i)}\right)^{\mathrm{I}} d_k^{\mathrm{Q}}\right)^2 + \left(\sqrt{\frac{\gamma}{N_t}}\left(h_{p_k}^{(i)}\right)^{\mathrm{Q}} d_k^{\mathrm{I}}\right)^2 + \left(n_{p_k}^{\mathrm{I}}\right)^2 + \left(n_{p_k}^{\mathrm{Q}}\right)^2 + g_{p_k}\right] \\
&= \sum_{k=1}^{2}\left\|\sqrt{\frac{\gamma}{N_t}}\mathbf{h}_k^{(i)} d_k\right\|^2 + \sum_{k=1}^{2}\|\mathbf{n}_k\|^2 + g.
\end{aligned} \tag{A2}$$

In (A2), $g = \sum_{k=1}^{2}\sum_{p=1}^{N_r} g_{p_k}$ and the Gaussian RVs $g_{p_k}, k \in [1{:}2], p \in [1{:}N_r]$, are given by

$$\begin{aligned}
g_{p_k} = \; & 2\sqrt{\frac{\gamma}{N_t}}\left(h_{p_k}^{(i)}\right)^{\mathrm{I}} n_{p_k}^{\mathrm{I}} d_k^{\mathrm{I}} - 2\sqrt{\frac{\gamma}{N_t}}\left(h_{p_k}^{(i)}\right)^{\mathrm{Q}} n_{p_k}^{\mathrm{I}} d_k^{\mathrm{Q}} \\
& + 2\sqrt{\frac{\gamma}{N_t}}\left(h_{p_k}^{(i)}\right)^{\mathrm{I}} n_{p_k}^{\mathrm{Q}} d_k^{\mathrm{Q}} + 2\sqrt{\frac{\gamma}{N_t}}\left(h_{p_k}^{(i)}\right)^{\mathrm{Q}} n_{p_k}^{\mathrm{Q}} d_k^{\mathrm{I}}
\end{aligned} \tag{A3}$$

and have mean $\mathcal{E}\left\{g_{p_k}\right\} = 0$ and variance

$$\begin{aligned}
\mathcal{E}\left\{g_{p_k}^2\right\} = \; & 2\left(\sqrt{\frac{\gamma}{N_t}}\left(h_{p_k}^{(i)}\right)^{\mathrm{I}} d_k^{\mathrm{I}}\right)^2 + 2\left(\sqrt{\frac{\gamma}{N_t}}\left(h_{p_k}^{(i)}\right)^{\mathrm{Q}} d_k^{\mathrm{Q}}\right)^2 \\
& + 2\left(\sqrt{\frac{\gamma}{N_t}}\left(h_{p_k}^{(i)}\right)^{\mathrm{I}} d_k^{\mathrm{Q}}\right)^2 + 2\left(\sqrt{\frac{\gamma}{N_t}}\left(h_{p_k}^{(i)}\right)^{\mathrm{Q}} d_k^{\mathrm{I}}\right)^2 \\
= \; & 2\left|\sqrt{\frac{\gamma}{N_t}} h_k^{(i)} d_k\right|^2.
\end{aligned} \tag{A4}$$

Thus, the distribution of the Gaussian RV g is given by $g \sim \mathcal{N}\left(0, \sigma_g^2\right), k \in [1{:}2]$, and $\sigma_g^2 = 2\sum_{k=1}^{2}\left\|\sqrt{\frac{\gamma}{N_t}}\mathbf{h}_k^{(i)} d_k\right\|^2$. This produces the same result as Xu et al,[8] and so (A1) may be expressed as follows:

$$
\begin{aligned}
P\left(\mathbf{L}\to\tilde{\mathbf{L}}|\mathbf{H}_1,\mathbf{H}_2\right) &= P\left(\sum_{k=1}^{2}\left\|\sqrt{\frac{\gamma}{N_t}}\mathbf{h}_k^{(i)}d_k\right\|^2+g<0\right)\\
&= Q\left(\frac{\sum_{k=1}^{2}\left\|\sqrt{\frac{\gamma}{N_t}}\mathbf{h}_k^{(i)}d_k\right\|^2}{\sigma_g}\right)\\
&= Q\left(\frac{1}{\sqrt{2}}\sum_{k=1}^{2}\left\|\sqrt{\frac{\gamma}{N_t}}\mathbf{h}_k^{(i)}d_k\right\|\right).
\end{aligned}
\tag{A5}
$$

Using the intermediate steps of (A2), the argument of the Q-function in (A5) is squared to produce (A6).

$$
\begin{aligned}
&\frac{1}{2}\sum_{k=1}^{2}\left\|\sqrt{\frac{\gamma}{N_t}}\mathbf{h}_k^{(i)}d_k\right\|^2\\
&=\frac{\gamma}{2N_t}\sum_{k=1}^{2}\sum_{p=1}^{N_r}\left[\left(\left(h_{p_k}^{(i)}\right)^{\mathrm{I}}d_k^{\mathrm{I}}\right)^2+\left(\left(h_{p_k}^{(i)}\right)^{\mathrm{Q}}d_k^{\mathrm{Q}}\right)^2+\left(\left(h_{p_k}^{(i)}\right)^{\mathrm{I}}d_k^{\mathrm{Q}}\right)^2+\left(\left(h_{p_k}^{(i)}\right)^{\mathrm{Q}}d_k^{\mathrm{I}}\right)^2\right]\\
&=\frac{\gamma}{2N_t}\sum_{k=1}^{2}\sum_{p=1}^{N_r}\left[\left(\left(h_{p_k}^{(i)}\right)^{\mathrm{I}}\right)^2|d_k|^2+\left(\left(h_{p_k}^{(i)}\right)^{\mathrm{Q}}\right)^2|d_k|^2\right].
\end{aligned}
\tag{A6}
$$

Since both the in-phase and quadrature components of fading follow Gaussian distributions, the Q-function in (A5) is expressed using the results of (A6) as follows:

$$
Q\left(\frac{1}{2}\sum_{k=1}^{2}\left\|\sqrt{\frac{\gamma}{N_t}}\mathbf{h}_k^{(i)}d_k\right\|\right)=Q\left(\sqrt{\sum_{p=1}^{N_r}\left(\alpha_{p_1}^2+\alpha_{p_2}^2+\alpha_{p_3}^2+\alpha_{p_4}^2\right)}\right),
\tag{A7}
$$

where the Gaussian RVs $\alpha_{p_1},\alpha_{p_2},\alpha_{p_3}$ and $\alpha_{p_4}, p\in[1{:}N_r]$, are defined by

$$
\alpha_{p_{(2k-1)}}=\frac{\sqrt{\gamma}|d_k|}{\sqrt{2N_t}}\left(h_{p_k}^{(i)}\right)^{\mathrm{I}},\quad k\in[1{:}2]
\tag{A8}
$$

$$
\alpha_{p_{(2k)}}=\frac{\sqrt{\gamma}|d_k|}{\sqrt{2N_t}}\left(h_{p_k}^{(i)}\right)^{\mathrm{Q}},\quad k\in[1{:}2]
\tag{A9}
$$

and have the distributions given in (11) to (14).